

Structure of partly dispersed normal shock waves in vapor-droplet flows

A. Guha

Whittle Laboratory, University of Cambridge, Madingley Road, Cambridge CB3 0DY, England

(Received 2 October 1991; accepted 10 March 1992)

A numerical and analytical study has been made to reveal the internal structures of partly dispersed shock waves in pure vapor-droplet media. The results clearly demonstrate the effects of different relaxation phenomena present and their associated time scales on the structure. The study systematically analyzes the relative effects of different flow parameters on the structure and thickness of the shock wave. Wherever possible, the structure in a vapor-droplet medium is contrasted against similar structures in more familiar solid particle-laden gas flow. The case of complete evaporation through which a two-phase vapor-droplet medium reverts to a single-phase nonrelaxing one is discussed. Although linearized analyses are often presented for relaxing flows downstream of frozen shocks, they are of limited applicability to vapor-droplet flows. The paper gives many examples of why a linearized analysis is unlikely to be successful in such cases.

I. INTRODUCTION

A partly dispersed shock wave can be described as a steep-fronted discontinuity, dominated by viscous dissipation and thermal conduction, followed by a continuous relaxation zone.¹ (The fluid goes out of equilibrium as it passes through the near discontinuity, called the frozen shock, and gradually returns to equilibrium in the relaxation zone. See Appendix A.) These type of waves in vapor-droplet flows are of great importance, both from the theoretical and practical point of view, as they often appear in the flow field if the upstream velocity is higher than the local frozen speed of sound² (which is the speed of sound in the vapor phase alone when all interaction with the liquid droplets are frozen). In converging-diverging nozzle flows with certain inlet conditions, such shock waves interact with the nucleation zone and give rise to an oscillatory flow pattern.^{3,4} It is probable that similar unsteadiness is also present in the last few stages of a real steam turbine used for electrical power generation where the maximum Mach number might be about 2. Such unsteadiness suggests a possible aerodynamic origin of the extra "wetness loss" observed in the nucleating stage of a turbine. Thus it is important to understand the detailed physics involved in the processes controlling the formation of such shock waves and this constitutes the subject of the present paper.

In this context, a vapor-droplet medium is considered to be a homogeneous, two-phase mixture of the continuous vapor phase and a large number of very small droplets (typically of radii less than $2\ \mu\text{m}$). The mixture is assumed to be pure, which means that the vapor and the liquid phases are of the same chemical species. The small size of the droplets ensures that surface tension maintains droplet sphericity in most situations. Sufficient number density and uniform distribution of the droplets make their interaction with the vapor describable by a continuous variation. Thus two-phase flows of this type respond well to mathematical modeling and the analysis applies to most wet vapor flows

formed initially by homogeneous nucleation and having wetness fractions less than about 0.2.

The general behavior of condensing flows were examined by Marble⁵ and Jackson and Davidson.⁶ Partly dispersed waves were discussed by Konorski⁷ and Bakhtar and Yousif,⁸ although these authors did not include any attempt at generalization. The relaxation processes in pure vapor-droplet flows and the structure of fully dispersed waves (which results when the upstream velocity lies between the frozen and equilibrium speed of sound) were studied by Young and Guha.⁹ Guha¹⁰ gave the Rankine-Hugoniot relations applicable to normal shock waves in vapor-droplet flows and analyzed the unsteady processes through which the shock waves attain their stable structure.² Reference 2 also contains a lucid and fairly detailed overview of the complex physics governing the shock-wave phenomena in vapor-droplet systems. There are also many references on the structure of dispersed waves in other types of flow. For example, Becker and Böhme¹¹ studied the structure of shock waves in relaxing gases for general thermodynamic behavior, Johannesen *et al.*¹² discussed vibrational relaxation regions in carbon dioxide, Nayfeh¹³ analyzed shock structure in a gas containing ablating particles, and Rudinger¹⁴ discussed the same for gas flows carrying small solid particles. Measurements of shock propagation in a shock tube have also been performed by Goossens *et al.*¹⁵ in the case of moist air and by Roth and Fischer¹⁶ in the case of aerosol droplet evaporation in argon.

Linearized analyses are often presented for relaxing flows downstream of frozen shocks (e.g., Ref. 1). The following results amply demonstrate why such a linearized analysis does not work well for vapor-droplet flows. Although the numerical calculations have been performed here specifically for wet steam, the formulas derived and the conclusions deduced are also valid for other vapor-droplet mixtures.

II. CONSERVATION EQUATIONS AND SOLUTION PROCEDURE

The basic one-dimensional gas-dynamic equations for steady, non-nucleating, constant-area-duct flow for a vapor-droplet system can be written in the usual way:

droplet number conservation:

$$\frac{d}{dx} (N_i V_{li}) = 0, \quad \text{for each droplet group;} \quad (1)$$

continuity:

$$\frac{d}{dx} (\rho_g V_g) + \sum \frac{d}{dx} (N_i m_i V_{li}) = 0; \quad (2)$$

momentum:

$$\frac{dp}{dx} + \frac{d}{dx} (\rho_g V_g^2) + \sum \frac{d}{dx} (N_i m_i V_{li}^2) = 0; \quad (3)$$

energy:

$$\frac{d}{dx} \left[\left(h_g + \frac{V_g^2}{2} \right) \rho_g V_g \right] + \sum \frac{d}{dx} \left[\left(h_{li} + \frac{V_{li}^2}{2} \right) N_i m_i V_{li} \right] = 0, \quad (4)$$

where p is the pressure, ρ is the density, h is the specific enthalpy, V is the velocity, and x is the distance along the flow direction. The subscript g denotes the vapor phase and subscript l refers to the liquid properties, neither of which are necessarily at saturation conditions. The summation sign here indicates summation over all the droplet groups, where the continuous distribution of droplet sizes is discretized into a number of groups such that the i th group contains N_i droplets of mass m_i per unit volume of the mixture. Since a monodispersed droplet spectrum will be assumed in the present analysis, there is only one droplet group present, and for convenience the subscript i will be dropped henceforth. However, since the algebra remains exactly the same, all the conservation equations that follow can be converted to deal with a polydispersed droplet spectrum simply by inserting a summation sign before each term that contains a contribution from the droplets.

The analysis is restricted to pure substances (so that phase change is heat transfer rather than diffusion controlled) and to low wetness fractions ($y < 0.2$) so that the volume occupied by the liquid phase is negligible. Also neglected is the partial pressure of the droplet cloud. The temperature T_l is assumed uniform throughout a droplet. (For well-established droplets, T_b at equilibrium, is close to the saturation temperature T_s . For example, the Kelvin-Helmholtz equation shows that, in a steam-water mixture, $T_s - T_l = 0.43$ °C if the droplet radius r is 0.05 μm , $T_s - T_l = 0.01$ °C if $r = 2.0$ μm .) We adopt the usual "two-fluid" model and view the droplets as providing sources or sinks of mass, momentum, and energy for the vapor, each source term varying continuously in the x direction. Coagulation as well as fragmentation of droplets is neglected. Indeed, for the types of flow considered here, the Weber number criterion for stability against fragmentation is well satisfied even for strong shock-wave deceleration. In passing through a shock wave, each droplet is therefore as-

sumed to retain its identity and individual droplet radii change solely by pure evaporation or condensation.

The wetness fraction y is then given by

$$y = n \cdot m, \quad (5)$$

where there are n droplets of mass m per unit mass of the mixture. The mass of an individual droplet is connected to its radius r , and the liquid density ρ_l via $m = 4/3\pi r^3 \rho_l$. If the vapor density is ρ_g , the mixture density (neglecting the volume of the liquid phase) is $\rho_g/(1-y)$ and the number of droplets per unit volume is given by

$$N = n\rho_g/(1-y). \quad (6)$$

We assume that the vapor phase behaves as a perfect gas with constant isobaric specific heat capacity c_p . Thus

$$\frac{d}{dx} \left(\frac{p}{\rho_g R T_g} \right) = 0 \quad (7)$$

and

$$\frac{dh_g}{dx} = c_p \frac{dT_g}{dx}, \quad (8)$$

where R is the specific gas constant and T_g is the temperature of the vapor. The perfect gas approximation is not crucial to the analysis (although this assumption is not far from reality for steam at low pressure, which is of more interest here). More realistic equations of state can be introduced if desired but these tend to complicate the algebraic development and do not provide any further physical insight.

Later, we shall specify the thermal equilibrium state by the saturation temperature T_s rather than the pressure. The two are related by the Clausius-Clapeyron equation. Neglecting the specific volume of the liquid and introducing the perfect gas equation for the vapor phase, we have

$$\frac{1}{p} \frac{dp}{dx} = \left(\frac{h_{fg}}{RT_s} \right) \frac{1}{T_s} \frac{dT_s}{dx}, \quad (9)$$

where h_{fg} is the specific enthalpy of evaporation and is a known function of temperature.

After considerable algebraic manipulation, the above continuity, momentum, and energy equations (2)–(4) can be put into the form (in the same order)

$$\rho_g \frac{dV_g}{dx} + V_g \frac{d\rho_g}{dx} + N V_l \frac{dm}{dx} = 0, \quad (10)$$

$$\frac{dp}{dx} + \rho_g V_g \frac{dV_g}{dx} + N m V_l \frac{dV_l}{dx} - \Delta V N V_l \frac{dm}{dx} = 0, \quad (11)$$

$$\begin{aligned} \rho_g V_g \frac{dh_g}{dx} + N m V_l \frac{dh_l}{dx} - V_g \frac{dp}{dx} \\ = (h_g - h_l) N V_l \frac{dm}{dx} - \frac{(\Delta V)^2}{2} N V_l \frac{dm}{dx} + N m \Delta V V_l \frac{dV_l}{dx}, \end{aligned} \quad (12)$$

where ΔV is the slip velocity given by $\Delta V = V_g - V_l$.

Substituting Eqs. (7), (8), and the relation $dh_l/dx = c_l dT_l/dx$, Eqs. (10)–(12) may be recast as three linear

simultaneous differential equations involving the three quantities dV_g/dx , dp/dx , and dT_g/dx . The latter may be solved for by a Gaussian elimination procedure if all other terms are known. However, as it stands, the equation set (1) and (10)–(12) is incomplete and must be supplemented by three equations representing the interphase transport of mass, momentum, and energy. The interphase transfer mechanisms are quantified in terms of relaxation times that represent the rates at which the two-phase system reverts to equilibrium following a disturbance. Three different relaxation processes can be identified in a vapor-droplet mixture.² As nonequilibrium variables, we choose $\Delta V = V_g - V_l$ to represent velocity (or inertial) relaxation, $\Delta T_l = T_s - T_l$ to represent droplet temperature relaxation, and $\Delta T = T_s - T_g$ to represent vapor thermal relaxation. (Note that ΔT represents the negative of the vapor superheat.) It is shown in detail in Ref. 9 that the interphase transfer equations can then be written,

$$\frac{dV_l}{dt_l} = \frac{\Delta V}{\tau_I}, \quad (13)$$

$$\frac{dT_l}{dt_l} = \frac{\Delta T_l}{\tau_D}, \quad (14)$$

$$(h_g - h_l)n \frac{dm}{dt_l} = \frac{(1-y)c_p \Delta T}{\tau_T} + \frac{y c_l \Delta T_l}{\tau_D}, \quad (15)$$

where $d/dt_l = V_l d/dx$ is the substantive derivative following the droplets and c_p and c_l are the vapor and liquid isobaric specific heat capacities. Equation (1) may also be written explicitly as

$$\frac{dN}{dx} = -\frac{N}{V_l} \frac{dV_l}{dx}. \quad (16)$$

The three relaxation times, viz., the inertial relaxation time τ_I , the droplet temperature relaxation time τ_D , and the vapor thermal relaxation time τ_T are given by⁹

$$\tau_I = (2r^2 \rho_l / 9 \mu_g) [\phi(\text{Re}) + 4.5 \text{ Kn}], \quad (17)$$

$$\tau_D = \left(\frac{RT_s}{h_{fg}} \right)^2 \left(\frac{r \rho_l c_l}{6R} \right) \frac{\sqrt{2\pi RT_s}}{p}, \quad (18)$$

$$\tau_T = [(1-y)c_p \rho_l r^2 / 3 \lambda_{g,v}] (1 + 4.5 \text{ Kn}/\text{Pr}), \quad (19)$$

where $\phi(\text{Re})$ is an empirical correction for large slip Reynolds numbers ($\text{Re} = 2\rho_g r |\Delta V| / \mu_g$) given by

$$\phi(\text{Re}) = [1 + 0.15 \text{ Re}^{0.687}]^{-1} \quad (20)$$

and λ_g and μ_g are the vapor thermal conductivity and dynamic viscosity, respectively. Here, Pr is the vapor Prandtl number and $\text{Kn} = l_g/2r$ is the droplet Knudsen number, l_g being the molecular mean-free path of the vapor and r the radius of the droplet. Young and Guha⁹ have discussed, at length, the assumptions involved in the derivation of the relaxation times and have indicated their range of validity. Equations (17)–(19) are supposedly valid for all droplet Knudsen numbers from the continuum to the free-molecule regime. For example, for small slip Reynolds numbers and continuum flow ($\text{Re} \ll 1$, $\text{Kn} \ll 1$), Eq. (17)

reduces to the Stokes drag formula for a sphere. For free-molecule flow ($\text{Kn} \gg 1$) an expression derivable from kinetic theory is obtained. The expression within the brackets in Eq. (17) provides a simple interpolation formula for intermediate Knudsen numbers. Similarly, for small Kn , Eq. (19) reduces to the continuum expression for steady-state heat transfer from a sphere. For large Kn , the kinetic theory (free-molecule) result is regained. The method of analysis is not dependent on the forms of (17)–(19), however, and other, possibly more suitable, expressions could easily be incorporated if desired.

Note that the equilibrium temperature in pure vapor-droplet flow is given by the saturation temperature T_s . Hence the temperatures of both phases have ultimately to fall or rise to the saturation value but they do so with different time scales. The droplet temperature approaches T_s with a time constant τ_D , whereas the vapor temperature approaches T_s with a time constant τ_T . Thus the reversion to thermal equilibrium following a disturbance usually takes place in two, almost independent, stages. Comparing the magnitudes of the three relaxation times given by Eqs. (17)–(19), it can be shown² that, in general, for a pure vapor-droplet mixture, $\tau_D \ll \tau_I \ll \tau_T$. Therefore, following a disturbance, on a very short time scale the droplet temperature reaches equilibrium, then the velocity slip and finally the vapor temperature relaxes to the equilibrium value.

Equations (10)–(16) give the spatial derivatives of the seven unknowns, viz., V_g , p , T_g , V_b , T_b , m , and N [y and n in the above equations may be calculated from Eqs. (5) and (6)]. They are integrated simultaneously by a fourth-order Runge–Kutta scheme until the departures from equilibrium become negligibly small (i.e., $\Delta T \rightarrow 0$, $\Delta V \rightarrow 0$). This equilibrium state then stands for the downstream condition of the entire shock wave. It should be noted that, for a polydispersed droplet spectrum, Eqs. (13)–(16) represent one set of four equations for each group of droplets.

At every step of the numerical integration procedure, Eqs. (13)–(16) are evaluated to give the values of dV_l/dx , dT_l/dx , dm/dx , and dN/dx as the nonequilibrium variables like ΔV , ΔT , etc., are known at the start of that step either from the calculations of the previous step or from a prescribed initial condition. Then the values of dV_g/dx , dp/dx , and dT_g/dx are determined by Gaussian elimination from Eqs. (10)–(12). Once the spatial derivatives of all the variables are known, they may be integrated numerically to calculate their respective values at the end of the step in consideration. This procedure is then repeated until equilibrium is established.

Out of the three relaxation processes, the droplet temperature equilibration is the fastest and hence is associated with the smallest relaxation time. Because of this small relaxation time, the step size required for accurate and stable explicit numerical integration is very small. Thus, to save computation time, as the droplet temperature becomes almost equal to its equilibrium value, T_l is set equal to the saturation temperature T_s . Equation (14) may then be dropped from the system of equations and Eq. (15) approximately becomes

$$\frac{dm}{dx} = \frac{(1-y)c_p \Delta T}{(h_g - h_l)nV_f \tau_T} \quad (21)$$

For other details of the solution procedure, one may refer to Ref. 17.

III. INITIAL CONDITIONS FOR NUMERICAL CALCULATION

For a computational procedure that marches forward in space, it is necessary to start from some initial condition that represents a deviation from equilibrium. Otherwise, out of the two possible downstream conditions that maintain the conservation of mass, momentum, and energy, the numerical procedure will give the trivial solution such that the far downstream condition is equal to the far upstream condition. For a partly dispersed wave (the upstream frozen Mach number being greater than unity), the initial condition for the above numerical integration procedure is straightforward. There is a frozen shock wave at the beginning and the vapor conditions just downstream of this frozen shock can be determined by applying the Rankine-Hugoniot relation for the vapor phase alone corresponding to the upstream frozen Mach number M_{f1} . [Frozen Mach number $M_f = V_g/a_f$, where the frozen speed of sound a_f is given by $a_f = \sqrt{(\gamma p/\rho_g)}$, and γ , for an ideal gas, is the ratio of two specific heats. The far upstream condition is denoted by the subscript 1.] The droplet parameters, e.g., radius, temperature, and velocity, are kept fixed at their respective upstream values (as the extent of the frozen shock is very small, the droplet parameters do not change appreciably as the droplets pass through the frozen shock). This gives the finite departure from equilibrium, which is necessary to start the numerical integration, at the downstream end of the frozen shock.

IV. AN ANALYTICAL STUDY OF THE EFFECTS OF DIFFERENT RELAXATION PHENOMENA

This section describes the qualitative variation of different thermodynamic properties of the vapor phase in the relaxation zone following a frozen shock, under the assumption that the departure from equilibrium is not too great.

If the second-order terms containing the products of the small quantities like $\Delta V/V_g$, $\Delta T/T_g$, $\Delta T_f/T_s$ are neglected, Eqs. (10)–(12) can be rearranged as

$$\frac{1}{V_g} \frac{dV_g}{dx} \left(1 - \frac{V_g^2}{a_f^2}\right) = \left(1 - \frac{c_p T_g}{h_{fg}}\right) \Theta - \frac{c_l T_s}{h_{fg}} \sigma + \frac{V_g^2}{a_f^2} \Pi, \quad (22)$$

$$\frac{1}{p} \frac{dp}{dx} \left(1 - \frac{V_g^2}{a_f^2}\right) = \frac{V_g^2}{RT_g} \left[-\left(1 - \frac{c_p T_g}{h_{fg}}\right) \Theta + \frac{c_l T_s}{h_{fg}} \sigma - \Pi \right], \quad (23)$$

$$\frac{1}{T_g} \frac{dT_g}{dx} \left(1 - \frac{V_g^2}{a_f^2}\right) = \left[1 - \frac{V_g^2}{RT_g} \left(1 - \frac{RT_g}{h_{fg}}\right) \right] \Theta + \frac{V_g^2}{c_p T_g} \frac{c_l T_s}{h_{fg}} \sigma - \frac{V_g^2}{c_p T_g} \Pi, \quad (24)$$

TABLE I. Influence table.

	Contribution from		
	Θ	Π	σ
dV_g/dx	negative	negative	negative
dp/dx	positive	positive	positive
dT_g/dx	neg./pos. ^a	positive	positive

^aPositive for $(V_g^2/RT_g)(1 - RT_g/h_{fg}) > 1$, negative for $(V_g^2/RT_g)(1 - RT_g/h_{fg}) < 1$.

where,

$$\Theta = \Delta T/V_g \tau_T T_g \quad (25)$$

$$\Pi = [y/(1-y)] (\Delta V/V_g \tau_I V_g), \quad (26)$$

$$\sigma = [y/(1-y)] (\Delta T_f/V_g \tau_D T_s). \quad (27)$$

The different variables Θ , Π , and σ represent the contributions from three relaxation phenomena taking place behind the frozen shock. Here, Θ is associated with vapor thermal relaxation, Π with inertial (or velocity slip) relaxation, and σ with droplet temperature relaxation. In a compression wave we have, $\Theta < 0$, $\Pi < 0$, $\sigma > 0$. In the relaxation zone following a discontinuity, $V_g < a_f$. Therefore we may construct the influence table as shown in Table I. Thus V_g always decreases and p always increases in the relaxation zone. (However, the conclusion regarding the variation of V_g may alter if nonlinear effects are taken into account, see Sec. V A and Appendix B.) If at the beginning of the relaxation zone $(V_g^2/RT_g)(1 - RT_g/h_{fg}) < 1$, T_g first increases as velocity slip dominates and then decreases as heat transfer takes over. The peculiar behavior of the vapor temperature with respect to heat transfer (variable Θ) bears close resemblance to the fact that, in single-phase ideal gas, heat removal results in an increase in the gas temperature in the flow regime $1 > M > 1/\sqrt{\gamma}$.

V. RESULTS OF NUMERICAL CALCULATION AND DISCUSSION

A. Variation of different flow parameters within the dispersed shock wave

Figure 1 shows the variation of different flow variables within a typical partly dispersed shock wave in wet steam, for upstream conditions given in the figure. After the frozen shock, the pressure continues to rise in the relaxation zone, at first quite rapidly and then at a decreasing rate. Since the pressure approaches asymptotically its far downstream equilibrium value, it actually takes quite a long distance before complete reversion to equilibrium is achieved. The vapor-phase velocity behaves in the same way as the pressure but in the opposite sense. It decreases discontinuously across the frozen shock and then continues to do so until it reaches the equilibrium value far downstream. The droplet velocity, on the other hand, does not change at all as it passes through the frozen shock and is always higher than the vapor-phase velocity inside the relaxation zone. The velocity slip equation [Eq. (13)] therefore indicates that the droplet velocity decreases monoton-

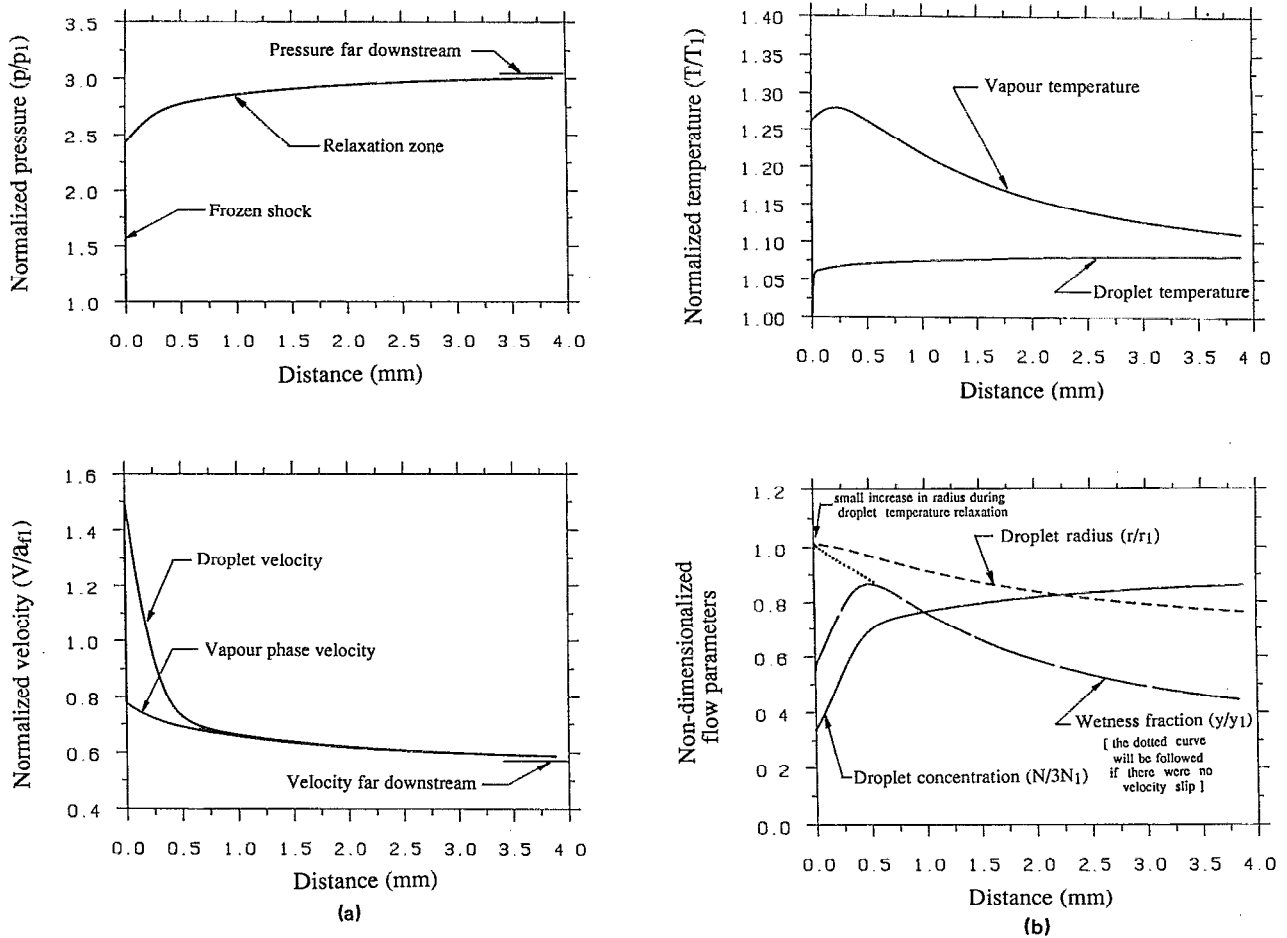


FIG. 1. Variation of different flow variables through a partly dispersed shock wave in wet steam ($M_{f1} = 1.5$, $r_1 = 0.1 \mu\text{m}$, $y_1 = 0.1$, $p_1 = 0.35 \text{ bar}$).

ically. However, it is interesting to note that, although the droplets move faster than the vapor, their drag does not accelerate the latter, and the vapor-phase velocity, in general, also decreases monotonically in the relaxation zone. This somewhat surprising result stems from the fact that, in compressible flow, all the conservation equations together with the equation of state have to be satisfied simultaneously. In doing so, the decrease due to pressure, for most cases, happens to exceed the increase due to droplet momentum transfer, so that the vapor-phase momentum also decreases. Of course, the vapor velocity has to decrease ultimately to a lower value, as the final equilibrium velocity is always less than the vapor-phase velocity just after the frozen shock,¹⁰ but that does not necessarily imply that it could not pass through an intermediate maxima. It can be shown (see Appendix B) that the vapor-phase velocity does decrease monotonically, at least so long as $M_{f1}^2 < 2\gamma/(\gamma - 1)$, a condition that is satisfied for most practical cases. (The subscript 1 refers to the far upstream condition before the frozen shock.)

In general, the droplet velocity decreases much faster than the vapor-phase velocity so that the slip velocity is progressively reduced. However, after a weak frozen shock, the vapor-phase velocity might decrease much more rapidly than the droplet velocity. It has been shown in

Appendix B that such a situation would arise if the upstream frozen Mach number is less than a limiting value, given by

$$M_{f1}^2 < [\gamma + 1 + y_1(\gamma - 1)] / (\gamma + 1 - 2y_1). \quad (28)$$

As a typical example, if we take $\gamma = 1.32$ and $y_1 = 0.1$, then the above relation gives $M_{f1} < 1.053$. A direct corollary of this condition is that the velocity slip and hence the drag continues to increase after the frozen shock and passes through an intermediate maximum. This surprising result is attributable to the fact that, within a range of Mach number, the inertial relaxation shows unstable behavior.² (See, for example, in Ref. 2 that this instability is the reason for the existence of Type II fully dispersed shock waves.) If the frozen shock is weak, then the vapor velocity just downstream of it may lie in this unstable region. Figure 2 clearly demonstrates the behavior of velocity slip for three different upstream frozen Mach numbers.

The vapor-phase temperature, on the other hand, does not show the monotonic behavior of the vapor-phase velocity and pressure. Initially, it increases (Fig. 1) as the pressure increases because of inertial relaxation and the fact that no significant interphase heat transfer has taken place so far. Physically, this might be attributed directly to

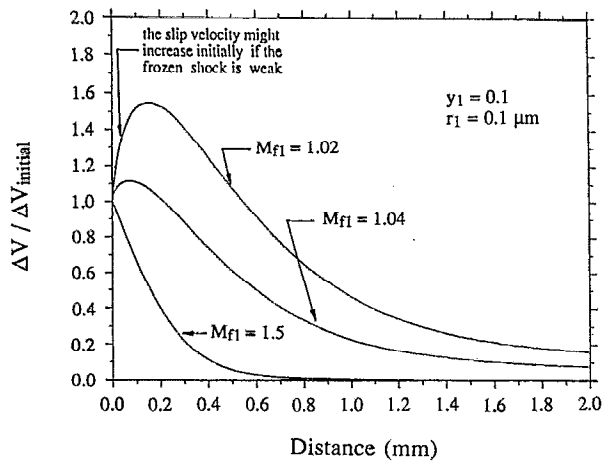


FIG. 2. Change in slip velocity through partly dispersed shock waves.

the frictional heating resulting from velocity slip (Sec. IV). Subsequently, however, the heat removed to supply the latent heat for the evaporation of the liquid droplets dominates and the vapor temperature starts to decrease until it reaches the saturation value corresponding to the pressure far downstream. In contrast, the droplet temperature increases monotonically as there is no mechanism that can bring its temperature above the saturation level (at least by the mathematical model of the droplet growth process we use). Initially, it starts with the saturation temperature corresponding to the pressure upstream of the frozen shock and, owing to the very short relaxation time involved, very quickly rises to the local saturation temperature. That means, in the whole relaxation zone, the vapor remains superheated and therefore the droplet radius decreases monotonically, as is evident from the droplet growth law [Eq. (21)]. However, inside the droplet temperature relaxation zone, Eq. (21) is not valid. There, both the heat transfer and mass transfer equations [Eqs. (14) and (15)] must be solved simultaneously. In fact, inside that zone, the molecular condensation rate exceeds the molecular evaporation rate. The resulting release of latent heat raises the droplet temperature to the local saturation value. Thus, within a very short zone, the radius increases slightly and from there onward decreases monotonically.

The variation of wetness fraction (Fig. 1) is more subtle in nature. Across the frozen shock, it decreases abruptly corresponding to the sudden jump in vapor density. This follows directly from the expression $y = Nm / (\rho_g + Nm)$, which is derivable from Eqs. (5) and (6). Across the frozen shock, m has not changed because no mass transfer has taken place, N also remains unchanged as the droplet velocity has not yet changed (droplet number conservation law). Therefore the wetness fraction decreases as ρ_g increases. Differentiating the expression for y , it can be shown that

$$dy = (m\rho_g dN + N\rho_g dm - Nm d\rho_g) / (\rho_g + Nm)^2.$$

As the droplet velocity always decreases in the relaxation zone, the droplet concentration per unit volume increases monotonically (physically, this means that the faster mov-

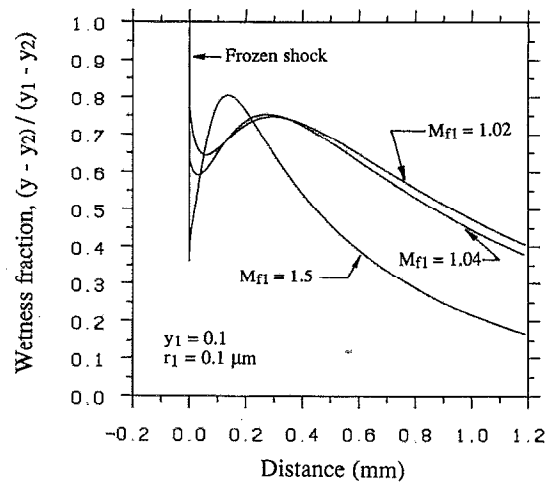


FIG. 3. Variation of wetness fraction through partly dispersed shock waves.

ing droplets are continually overtaking the slower moving vapor particles and also moving into a zone of higher vapor density). Thus, in the relaxation zone, $dN > 0$, $dm < 0$, $d\rho_g > 0$. Initially, the change of radius will be negligible, as that process is governed by a relatively large relaxation time. Therefore there are two opposing effects in the inertial relaxation zone (the zone of equilibration of the velocity slip): the change in droplet concentration trying to increase the wetness fraction and the change in vapor density tending to reduce it. To find the dominating process, set $dm \approx 0$, both in the continuity equation and also in the above expression for dy . Substituting $d\rho_g = -(\rho_g/V_g)dV_g$ [from continuity, Eq. (2)] and $dN = -(N/V_l)dV_l$ [droplet number conservation, Eq. (16)] in the expression for dy , it can be shown that the wetness fraction will increase, i.e., $dy > 0$, if $dV_g/V_g > dV_l/V_l$ (note both dV_g and dV_l are negative in general).

In Appendix B, it is shown that the critical Mach number for this condition to hold is given by the root of the equation

$$(\gamma - 1)M_{f1}^4 + [(3 - \gamma)(1 - y_1) - 2y_1\gamma]M_{f1}^2 - 2(1 - y_1) = 0.$$

For $\gamma = 1.32$ and a typical upstream wetness fraction of 0.1, this critical Mach number is found to be 1.058. Thus, if $M_{f1} > 1.058$, the wetness fraction increases downstream of the frozen shock; if $M_{f1} < 1.058$, the wetness fraction continues to decrease farther downstream of the frozen shock (Fig. 3). However, in the latter case, it soon passes through a local minimum, and increases again before decreasing ultimately because of interphase heat transfer. That, within the inertial relaxation zone where the velocity slip is equilibrated, there will be a region where the wetness fraction rises, can be seen by integrating the condition $dV_g/V_g > dV_l/V_l$ between the position just after the frozen discontinuity (denoted by subscript d) and that where velocity equilibrium is achieved (denoted by subscript v). Since $\ln(V_{gv}/V_{gd}) > \ln(V_{lv}/V_{ld})$ (as $V_{ld} > V_{gd}$ and $V_{lv} = V_{gv}$), the net change in wetness fraction across the inertial relaxation zone is positive. In fact, if it were possible to

freeze the change in droplet radius altogether, then the above process would bring the wetness level exactly to its initial value *before* the frozen shock. (This can be verified by applying the conservation laws across the frozen shock plus the inertial relaxation zone.) However, the above analysis is not valid throughout the inertial relaxation zone. After some distance downstream of the frozen shock, the change in radius becomes increasingly important (radius decreases because of evaporation). The wetness fraction therefore passes through a maximum and subsequently falls. It is important to realize that, although the wetness fraction changes in a complicated manner as a result of the slip between the two phases, the far upstream equilibrium wetness fraction is related to the far downstream equilibrium wetness fraction simply by the ratio of the mass of the droplets at the respective locations, as for steady flow, the number of droplets per unit mass of the mixture has to be the same at both locations (i.e., $n_1 = n_2$). This can be shown by writing the conservation equations between the far upstream (subscript 1) and far downstream (subscript 2) condition where full equilibrium is reestablished:

continuity:

$$\rho_{g1}V_1/(1-y_1) = \rho_{g2}V_2/(1-y_2);$$

droplet number:

$$N_1V_1 = N_2V_2;$$

by definition:

$$N_1 = y_1\rho_{g1}/m_1(1-y_1), \quad N_2 = y_2\rho_{g2}/m_2(1-y_2).$$

Combining these expressions and neglecting change in liquid density, $y_1/y_2 = m_1/m_2 \approx (r_1/r_2)^3$. Thus the overall change in wetness fraction is due only to the evaporation of the droplets. All of these different types of variation of wetness fraction through a partly dispersed shock wave are shown clearly in Fig. 3.

Figure 4 shows the variation of all the important variables (for the particular example of Fig. 1) suitably non-dimensionalized for plotting on the same graph. It clearly brings out the three relaxation processes involved and the associated time scales. The droplet temperature equilibration is accomplished over a very short distance and, in fact, could be merged together with the frozen shock, in the same way as the frozen shock was treated as a mathematical discontinuity ignoring the effects of viscosity and thermal conductivity. The velocity relaxation is practically complete within 1.0 mm of the frozen shock, whereas, even after 4 mm, there is a significant amount of residual superheating. This is, of course, expected, since the vapor thermal relaxation time is one order of magnitude higher than the inertial relaxation time in this example [$\tau_T/\tau_I \sim O(1/y)$, $y=0.1$]. If the situation in vapor-droplet systems as discussed here is compared with a typical partly dispersed shock wave in a solid-particle-laden gas,¹⁴ one may at once find at least four qualitative differences:

(1) In solid-particle-laden gases, there are only two relaxation zones (velocity and temperature) compared with three in vapor-droplet system.

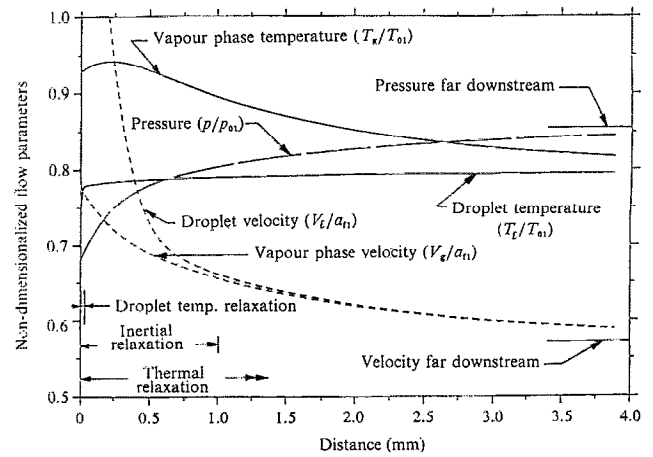


FIG. 4. Variation of different flow variables through a partly dispersed shock wave in wet steam ($M_{f1} = 1.5$, $r_1 = 0.1 \mu\text{m}$, $y_1 = 0.1$, $p_1 = 0.35 \text{ bar}$).

(2) In solid-particle-laden gases, no mass transfer is involved and the particle size remains constant. The relaxation process in wet vapor gets more complicated as the size of the droplets change continuously due to net evaporation. Thus the different relaxation times may vary significantly in the relaxation zone in the latter case.

(3) In solid-particle-laden gas flow, the inertial and thermal relaxation times are normally of the same order of magnitude, and hence the extent of the temperature and velocity relaxation zones are comparable.

(4) In wet vapor, the droplet temperature (and the final equilibrium temperature) is governed by the saturation temperature corresponding to the prevailing pressure. Hence, after the frozen shock, the major change occurs in the vapor temperature as it has to decrease to the saturation value. This is possible, even though the mass fraction of the vapor phase is much more than that of the droplets, because the latent heat of evaporation h_{fg} is very high compared to terms like $c_p\Delta T_g$. Thus the large amount of heat liberated by the cooling down of vapor can be absorbed by the evaporation of only a part of the liquid phase. In a solid-particle-laden gas, on the other hand, the gas temperature changes only slightly after the frozen shock (since the mass fraction of the gas phase is greater than that of the particles). The major change therefore occurs in the particle temperature, which has to rise to the level of the gas temperature by interphase heat transfer (Ref. 14, Fig. 1). (This may alter if the specific heat of the particles is significantly higher than that of the gas.)

B. Effects of different upstream parameters

The structure and thickness of partly dispersed shock waves depend on the various upstream parameters. The effects of each important upstream variable have been studied below in isolation while keeping the remaining variables fixed at specified average values. Some representative results are tabulated in Table II, the conclusions being summarized in Table III. In the following discussion we define shock thickness as the length over which the thermal

TABLE II. Illustration of typical numerical calculations.

Compare the effect of	Upstream variables			Length of inertial relaxation zone	Shock thickness	Just after the frozen shock				Far downstream			Average thermal relaxation time
	M_{f1}	r_1 (μm)	y_1	(mm)	(mm)	y_d	Kn	$\tau_{Td}/10^{-6}$ (sec)	$\tau_{Td}/10^{-7}$ (sec)	$\tau_{T2}/10^{-6}$ (sec)	y_2	r_2/r_1	$[(\tau_{Td} + \tau_{T2})/2]/10^{-6}$ (sec)
Radius	1.5	0.1	0.1	0.87	9.08	0.055	0.566	9.33	3.49	7.88	0.038	0.727	8.61
	1.5	0.5	0.1	10.83	104.62	0.055	0.113	100.44	33.19	89.84	0.038	0.727	95.12
	1.5	1.0	0.1	36.77	384.77	0.055	0.057	362.50	92.25	331.70	0.038	0.727	347.10
Wetness fraction	1.5	0.1	0.08	0.84	15.26	0.043	0.566	11.93	3.49	15.06	0.016	0.582	13.49
	1.5	0.1	0.1	0.87	9.08	0.055	0.566	9.33	3.49	7.88	0.038	0.727	8.61
	1.5	0.1	0.13	0.89	5.64	0.072	0.566	6.44	3.49	3.49	0.067	0.802	4.97
	1.5	0.1	0.2	0.86	2.74	0.115	0.566	4.15	3.49	2.2	0.14	0.887	3.17
Frozen Mach no.	1.2	0.1	0.1	2.44	12.31	0.076	0.746	9.64	5.02	7.33	0.07	0.887	8.49
	1.5	0.1	0.1	0.87	9.08	0.055	0.566	9.33	3.49	7.88	0.038	0.727	8.61
	1.7	0.1	0.1	0.65	11.96	0.046	0.495	9.04	2.87	17.17	0.008	0.439	13.10

nonequilibrium ΔT has decreased to 1% of the initial departure. Similarly, the inertial relaxation length is defined as the distance over which ΔV has decreased to 1% of its initial value.

1. Effect of droplet radius

The relaxation times depend strongly on the droplet radius. From common sense, it can be argued that if a droplet is bigger, it will have more inertia to retain its current properties and hence deviations from equilibrium will be greater. An alternative, but equivalent, view is that a larger droplet radius (for the same wetness fraction) implies a smaller number of droplets and less total surface area through which momentum and heat transfer take place. The consequence is that, for the same initial departure from equilibrium, larger droplets require a longer distance to return to equilibrium, and hence the shock thickness is larger. To ascertain the exact dependence, consider the expression [Eq. (19)] for the vapor thermal relaxation time (which has the strongest influence in determining the shock thickness): If $Kn \gg 1$ (free-molecular regime),

$$\tau_T \propto r \quad (\text{if } y \text{ is const});$$

if $Kn \ll 1$ (continuum regime),

$$\tau_T \propto r^2 \quad (\text{if } y \text{ is const}).$$

Thus the shock thickness is approximately proportional to the initial droplet radius in the free-molecule regime and is proportional to the square of the initial droplet radius in the continuum regime. Since in the illustration (Table II) $Kn \sim 1$, the dependence of shock thickness on radius lies between that for the free-molecule and the continuum regime.

Since the thermal and inertial relaxation times depend on the droplet radius, more or less, in the same way, the relative magnitudes of the inertial relaxation zone and the thermal relaxation zone remain almost the same. While writing the conservation equations between the far upstream and the far downstream equilibrium conditions, nowhere in the equations does the droplet radius occur as an independent parameter.¹⁰ Overall, changes across the shock wave depend only on the total quantity of the liquid phase present (viz., the wetness fraction) and not on its distribution. Hence the far downstream condition of the shock wave remains exactly the same independent of the radii of the droplets.

TABLE III. Summary of the influence of the different upstream parameters on the structure of shock wave.

Increase in upstream variables	Initial departure from equilibrium	Final equilibrium conditions	Shock thickness	Inertial relaxation length/thermal relaxation length
Frozen Mach no.	<i>increases</i>	<i>changes pressure \uparrow velocity \downarrow</i>	<i>might decrease or increase</i>	<i>generally decreases as the inertial relaxation length decreases</i>
Droplet radius	<i>no change</i>	<i>no effect</i>	<i>Increases free molecule: $\propto r$ continuum: $\propto r^2$</i>	<i>no appreciable change</i>
Wetness fraction	<i>no change</i>	<i>changes pressure \uparrow velocity \downarrow</i>	<i>decreases faster than $\propto 1/y$</i>	<i>increases inertial relaxation tends to become as important as thermal</i>

2. Effect of wetness fraction

Since $\tau_T/\tau_I = O(1/y)$, a change in wetness fraction implies a change in the relative magnitudes of the two relaxation times. Since the inertial relaxation time is independent of the wetness fraction, inertial equilibrium is attained almost at the same place irrespective of the upstream wetness fraction. However, although $\tau_T \propto 1/y$, the overall shock thickness does not vary according to the same relation. Table II shows that, as the wetness fraction is decreased by 2.5 times (from 0.2 to 0.08), the shock thickness increases by 5.5 times (from 2.74 to 15.26 mm). There are two reasons for this:

(1) τ_T varies significantly through the shock wave, as shown in Fig. 5. (Incidentally, this is one of the reasons why a linearized analysis of the relaxation zone does not give good results, which assumes τ_T to be constant. The variation of different relaxation times from point to point in the flow field, on the other hand, can easily be accommodated in a numerical integration procedure. Another major reason for the failure of linear analysis is given in Appendix C.) The initial decrease of τ_T after the frozen shock is due to the increase in wetness fraction as a result of inertial relaxation. Subsequently, τ_T increases as a result of evaporation. It can be easily shown [from Eq. (19)] that, after velocity equilibrium is obtained [when $V_g = V_b$, Eqs. (1), (2), and (6) together would give $dn/dx = 0$], the rate of change of τ_T in the relaxation zone is given by:

$$\frac{d\tau_T}{dx} \propto \frac{d}{dx} \left(\frac{1}{r} \right) \quad \text{in continuum flow (Kn} \ll 1),$$

$$\frac{d\tau_T}{dx} \propto \frac{d}{dx} \left(\frac{1}{r^2} \right) \quad \text{in free-molecule flow (Kn} \gg 1).$$

Thus the variation of τ_T depends on how fast the droplet radius changes as a result of evaporation.

(2) As y increases, the thermal relaxation zone becomes comparable with the inertial one and it is no longer the thermal relaxation time alone that controls the overall thickness but a complicated combination of τ_T and τ_I that governs the relaxation length.

It has been shown by Guha¹⁷ that, in the continuum regime $\tau_{T2}/\tau_{Td} \approx \rho_{g1}/\rho_{gd} \cdot r_1/r_2$, and in the free-molecule regime $\tau_{T2}/\tau_{Td} \approx \rho_{g1}/\rho_{gd} \cdot (r_1/r_2)^2$, where the suffices 1, d , and 2 refer to "far upstream," "just after the frozen discontinuity" and "far downstream," respectively. From classical Rankine-Hugoniot analysis, the ratio ρ_{g1}/ρ_{gd} is a function of upstream frozen Mach number M_{f1} only. The radius ratio across the shock, r_1/r_2 , is given by $r_1/r_2 = \sqrt[3]{y_1/(y_1 - \Delta y)}$, where the net evaporation Δy is also predominantly a function of M_{f1} . (This can easily be seen from Table II. A theoretical argument for why it is so is given in Ref. 10.) Since the wetness fraction varies as (radius)³, for the same net change of wetness fraction (constant $\Delta y = y_1 - y_2$), the ratio r_2/r_1 decreases rapidly for values of y_1 of the order of Δy , as shown in Fig. 6. Thus, keeping M_{f1} fixed, if y_1 is lowered sufficiently, r_2/r_1 may attain a very low value and τ_{T2} may increase greatly over τ_{Td} (Fig. 5). A study of Table II will also illustrate this

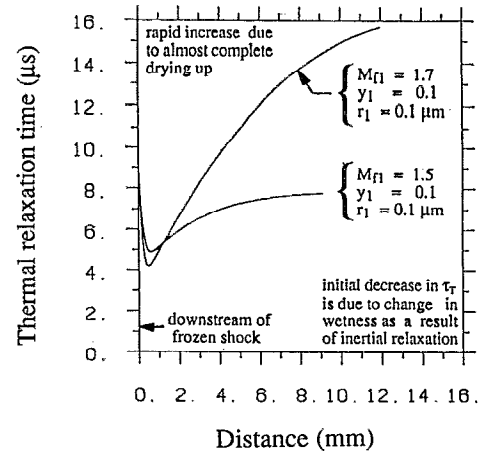


FIG. 5. Variation of vapor thermal relaxation time τ_T through shock waves.

point. As a result of this large increase in τ_T due to evaporation, the average relaxation time over the whole relaxation zone may be significantly higher than its initial value. Thus, for decreasing initial wetness fraction y_1 , the shock thickness increases at a faster rate than $1/y_1$. (Note that the ratio r_2/r_1 does not depend on the initial radius r_1 , and, consequently, τ_{T2}/τ_{Td} is also almost independent of r_1 .)

In contrast to the effect of droplet radius, the downstream equilibrium condition does depend on the upstream wetness fraction. Since, for the same upstream frozen Mach number, an increase in wetness fraction means a higher upstream equilibrium Mach number, the downstream pressure increases with a corresponding decrease in velocity.¹⁰

3. Effect of upstream frozen Mach number

The initial departure from equilibrium varies as the strength of the frozen shock alters due to a change in up-

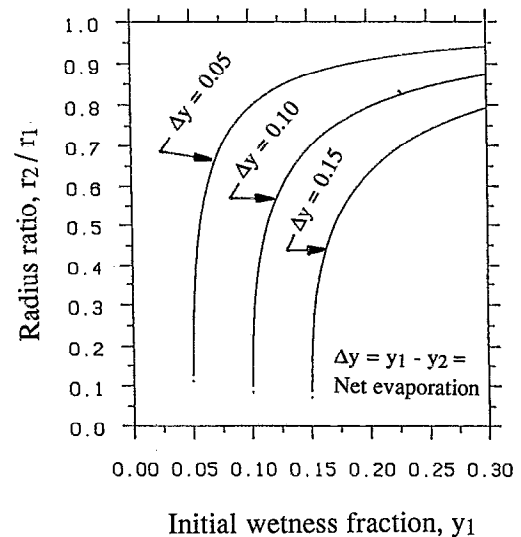


FIG. 6. Change in droplet radius across shock waves.

stream frozen Mach number M_{f1} . For a solid-particle-laden gas flow, a stronger frozen shock is normally associated with a reduction in shock thickness. This is because, for the same upstream pressure and temperature, a stronger frozen shock means a lower downstream velocity. Therefore the shock thickness, which is proportional to (velocity \times relaxation time), decreases. Thus, although reversion to equilibrium (say, within 1% of initial departure) takes the same amount of time, it occurs over a shorter distance because of the lower velocity. For a vapor-droplet flow, however, the situation is more complicated as the relaxation times are not independent of the strength of the frozen shock. Consider first the inertial relaxation time. Since this depends on the Reynolds number corresponding to the slip velocity, it decreases with increasing frozen Mach number. This further strengthens the effect of lower downstream velocity, and hence the inertial relaxation length is always less for higher upstream frozen Mach numbers. Similar effects would be observed in solid-particle-laden gas flow as well.

A very different picture exists for the vapor thermal relaxation time. Although the wetness level just downstream of the frozen shock decreases substantially with increasing frozen Mach number M_{f1} , the vapor thermal relaxation time just after the frozen shock, τ_{Td} , may not change appreciably as the Knudsen number also decreases (I_g decreases because of the higher pressure) and, consequently, the dependence of τ_T on radius changes. [Other properties in Eq. (19) also change slightly depending on the strength of the frozen shock. In either of the limits $Kn \ll 1$ or $Kn \gg 1$, the above effect of varying Knudsen number would be negligible and τ_{Td} would increase with rising M_{f1} .] However, since a stronger frozen shock leads to increased evaporation, the far downstream wetness fraction is lower for higher values of M_{f1} (the initial wetness fraction remaining the same). As already explained, this may give rise to a higher value of τ_{T2} downstream. There are, therefore, two opposing effects as M_{f1} increases. The lower downstream velocity tends to decrease the shock thickness whereas the increased τ_{T2} tends to increase it. Thus, as M_{f1} increases, the overall shock thickness may decrease or increase, depending on which of the above two effects predominate. Table II shows that, for $M_{f1} = 1.5$, $r_1 = 0.1 \mu\text{m}$, and $y_1 = 0.1$, the shock thickness is 9.08 mm. Keeping r_1 and y_1 fixed, as M_{f1} is either decreased to 1.2 or increased to 1.7 (in this case almost complete evaporation takes place, as is evident from the value of y_2 far downstream), the shock thickness increases to 12.31 and 11.96 mm, respectively.

C. Complete evaporation within the dispersed shock wave

So far, we have discussed partly dispersed shock waves where both far upstream and far downstream, the vapor-droplet mixture was in equilibrium. However, if the upstream wetness fraction is insufficiently high, then, after a strong frozen shock, the liquid phase may evaporate completely within the relaxation zone. A peculiar situation thus arises: the two-phase system before the shock has been

converted to a single-phase system downstream of the shock! (This situation does not arise in the case of solid-particle-laden gas flow.) This is another example of the fact, which has already been stressed many times, that vapor-droplet flows, while retaining the major characteristics of a relaxing two-phase medium, is quite unique in its behavior. What happens in this case? After the frozen shock, the two-phase system relaxes in the usual way and the same numerical marching technique can be employed to find the variation of flow properties until there is no liquid phase left. There cannot be any further change in the vapor properties and therefore this constitutes the downstream condition of the entire shock wave corresponding to the given upstream frozen Mach number and wetness fraction. Although this apparently suggests that the space-marching calculations end rather abruptly, no discontinuity in the slope of the profile of various properties results. Such discontinuities in the slope could have resulted if the relaxation times were fixed. However, as the wetness fraction decreases, the vapor thermal relaxation time increases ($\tau_T \rightarrow \infty$, as $y \rightarrow 0$) and the different vapor properties approach their respective downstream values very smoothly [i.e., $d/dx (p, V_g, \text{ or } T_g) \rightarrow 0$ at the downstream end]. [It should be noted that the vapor temperature responds *simultaneously* to heat transfer from *all* droplets and thus all droplets are instrumental in raising or lowering the temperature to the saturation value. It is to represent this integrated effect of the droplet cloud that the wetness fraction enters the expression for vapor thermal relaxation time τ_T as in Eq. (19). The condition $\tau_T \rightarrow \infty$ as $y \rightarrow 0$ physically means that, in the absence of liquid phase, the vapor temperature at equilibrium is no longer constrained to the saturation temperature and the vapor may remain superheated.]

It is possible to establish the minimum upstream wetness level required for a given upstream frozen Mach number so that, after the dispersed shock, the vapor-droplet mixture remains marginally wet. For this, the different conservation equations must be applied across the shock¹⁰ and solved iteratively, subject to the boundary condition of $y_2 = 0$. This boundary line for wet steam is shown in Fig. 7. Although it was calculated for an initial pressure of 0.35 bar, it is quite insensitive to the absolute pressure level. For initial wetness fractions above this curve, the steam will be an equilibrium two-phase mixture at the downstream end of a partly dispersed shock wave. For initial wetness fraction below this curve, complete evaporation will take place inside the shock wave. It is to be noted that the minimum wetness fraction is not zero at $M_{f1} = 1$, in contrast to what has been shown by Konorski.⁷ This is because fully dispersed shock waves may exist for $M_{f1} < 1$, leading to evaporation of the liquid phase.

It is known that the same form of Rankine-Hugoniot relations as used for ideal gas can be applied to solid-particle-laden gas flow if the upstream *equilibrium* Mach number and a suitable γ for the mixture are used for such calculations.¹⁴ However, it has been shown in Ref. 10 that, although similar relations may be devised for weak shock waves in vapor-droplet flow, they cease to apply if com-

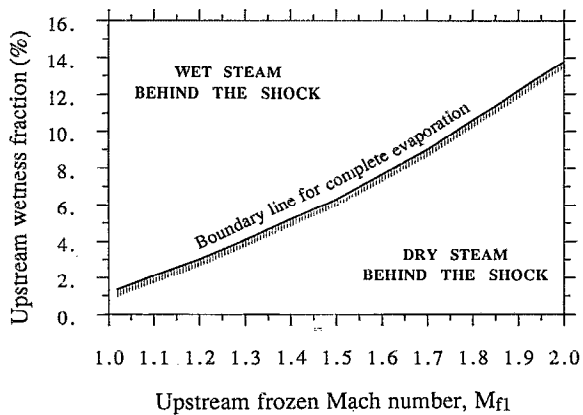


FIG. 7. Criterion for complete evaporation through a shock wave.

plete evaporation takes place and separate jump conditions have to be used then.

VI. CONCLUSIONS

The structure of partly dispersed shock waves in wet vapor has been analyzed in detail. The variation of different flow variables through the shock wave has been discussed and the limiting conditions for each type of variation to occur have been derived. An analytical theory has been developed in Sec. IV, which shows the role of different relaxation phenomena on the variation of vapor phase properties in the relaxation zone. The influence of different flow conditions on the structure and thickness of shock waves has been studied. Many peculiarities in the shock structure illustrate why a linear theory might not faithfully represent the relaxation zone. Some interesting and complicated features of partly dispersed shock waves in vapor-droplet flow have been elucidated and have been compared with the corresponding cases in solid-particle-laden gas flow. The case of complete evaporation has been discussed, which is the direct outcome of interphase mass transfer in vapor-droplet mixtures.

ACKNOWLEDGMENTS

The author is grateful to Dr. J. B. Young for his helpful comments on the manuscript and to Gonville and Caius College, Cambridge for awarding him a Research Fellowship.

APPENDIX A: RELAXATION PHENOMENA AND THE STRUCTURE OF SHOCK WAVES

If the value of some property of a medium is perturbed from its equilibrium value and the restoration to equilibrium occurs at a *finite rate*, the medium is called a relaxing medium and the process of restoration is termed relaxation. A relaxing medium such as a vapor-droplet mixture exhibits the property of frequency dispersion, i.e., the speed of a harmonic sound wave through the medium is a function of the frequency itself. If the frequency is very high, the sound wave travels through the medium such that all relaxation processes arising out of nonequilibrium mass,

momentum, and energy transfer between the two phases remain essentially frozen. The medium behaves like a single-phase vapor and the speed of sound in these situations is termed the frozen speed a_f . On the other hand, if the frequency of the harmonic sound wave is low, full equilibrium between the vapor and the liquid droplets is maintained always and the wave travels with the equilibrium speed of sound a_e . In general, $a_f > a_e$. Because of the dispersion in sound speed, two limiting Mach numbers can be defined corresponding to a particular flow velocity V : (i) a frozen Mach number $M_f = V/a_f$ and (ii) an equilibrium Mach number $M_e = V/a_e$. In general, $M_e > M_f$. As a result, two distinct types of shock waves might occur in such a medium. If the upstream velocity is higher than the frozen speed of sound ($M_{f1} > 1$), a discontinuity forms in the same way as an adiabatic shock forms in an ideal gas. Only vapor properties change across such (near) discontinuities and can be calculated using the classical Rankine-Hugoniot relations. Droplet properties such as temperature, radius, or velocity remain unaffected across the frozen shock. Hence the vapor-droplet medium is not at equilibrium downstream of the frozen shock. Interphase transport of mass, momentum, and energy, therefore, takes place in order to establish equilibrium and a relaxation layer develops. Such types of shock waves are called partly dispersed waves. If the upstream velocity lies in the range $(a_e)_1 < V_1 < (a_f)_1$, a fully dispersed wave may form where flow properties change *continuously* from one equilibrium state to another. For more details, see Ref. 2.

APPENDIX B: DETERMINATION OF DIFFERENT LIMITING MACH NUMBERS

The objective here is to obtain an expression for the rate of change of vapor-phase velocity in the vicinity of the frozen shock in relation to the rate of change of the droplet velocity. We shall consider the effect of velocity slip relaxation only, since this is the dominating mechanism in the present case of interest. For simplicity, therefore, two assumptions are made:

- (1) The droplet temperature is equal to the saturation temperature (and so terms like dh/dx will be neglected).
- (2) There is no effective mass transfer, i.e., $dm/dx=0$. This is close to the truth in the vicinity of the frozen shock because of the large thermal relaxation time.

In any case, the effect of both these terms is to decrease vapor-phase velocity (as shown in Sec. IV). Since we are interested in deducing whether or not the vapor-phase velocity might increase initially under certain circumstances, inclusion of these two small terms will probably change the magnitude of the limiting Mach number slightly, but the main conclusion nevertheless remains valid.

Under these assumptions, the conservation equations (10)–(12) become

continuity:

$$\rho_g \frac{dV_g}{dx} + V_g \frac{d\rho_g}{dx} = 0; \quad (B1)$$

momentum:

$$\frac{dp}{dx} + \rho_g V_g \frac{dV_g}{dx} + NmV_l \frac{dV_l}{dx} = 0; \quad (B2)$$

energy:

$$c_p \rho_g V_g \frac{dT_g}{dx} - V_g \frac{dp}{dx} = NmV_l \Delta V \frac{dV_l}{dx}. \quad (B3)$$

Note that Eqs. (B1)–(B3) are valid in the relaxation zone downstream of the frozen discontinuity. If the subscripts 1 and d refer to far upstream (before the frozen shock) and just after the frozen shock, respectively, then classical Rankine–Hugoniot relation gives $\rho_{gd} = \rho_{g1} V_1 / V_{gd}$. The vapor velocity V_{gd} is less than the local frozen speed of sound. The droplet velocity does *not* change as it passes through the frozen shock. Therefore $V_{ld} = V_{l1} = V_{g1} = V_1$. Droplet number conservation gives $N_1 V_1 = N_d V_{ld}$. Therefore $N_d = N_1$. The radii of the droplets also do not change during their passage through the frozen shock. Therefore $m_d = m_1$. Combining Eqs. (5) and (6), it can be shown that $N_d m_d / \rho_{gd} = [y_1 / (1 - y_1)] (V_{gd} / V_{ld})$. This relation is used while deriving Eqs. (B6) and (B8).

After systematic elimination of dp/dx and dT_g/dx from Eqs. (B1)–(B3), the system of equations reduces to

$$\left(\rho_g - \frac{\rho_g V_g^2}{RT_g} + \frac{p V_g^2}{RT_g^2 c_p} \right) \frac{dV_g}{dx} + \left(-\frac{NmV_l V_g}{RT_g} + \frac{NmV_l^2}{T_g c_p} \right) \frac{dV_l}{dx} = 0,$$

and hence

$$\frac{dV_g}{dV_l} = \frac{NmV_l V_g}{RT_g \rho_g} \cdot \frac{1}{(1 - M_f^2)} \cdot \left(1 - \frac{\gamma - 1}{\gamma} \cdot \frac{V_l}{V_g} \right), \quad (B4)$$

where γ is the isentropic exponent of the vapor phase and M_f is the frozen Mach number given by $M_f = V_g / \sqrt{\gamma RT_g}$.

1. Variation of vapor-phase velocity

It should be noted that all quantities in the above equation refer to the downstream condition of the frozen shock. Hence $(1 - M_f^2) > 0$, $dV_l < 0$. Therefore dV_g will be negative so long as $1 - (\gamma - 1)/\gamma \cdot V_l/V_g > 0$.

Note that the ratio V_l/V_g is also the ratio of the vapor velocities across the frozen shock (i.e., $V_{ld}/V_{gd} = V_{g1}/V_{gd}$). Relating the ratio V_l/V_g to the upstream frozen Mach number M_{f1} using the Rankine–Hugoniot equation, then the condition for vapor-phase velocity to decrease becomes

$$\frac{(\gamma + 1)M_{f1}^2}{(\gamma - 1)M_{f1}^2 + 2} < \frac{\gamma}{\gamma - 1},$$

which, after simplification, reduces to

$$M_{f1}^2 < 2\gamma / (\gamma - 1). \quad (B5)$$

With $\gamma = 1.32$, this relation implies that the vapor-phase velocity after a strong frozen shock might increase initially if the upstream frozen Mach number $M_{f1} > 2.9$. However, after such a strong shock, the initial superheat would be so high that heat transfer would become important even though the thermal relaxation time is large. The consequence is that the above limit would actually be greater than 2.9 and such a high Mach number does not normally occur in practice. It should also be noted that, if the second-order term containing ΔV was omitted in the energy equation (which a linear theory will do, as shown in Sec. IV), the conclusion would have been that, behind the frozen shock, the vapor-phase velocity decreases unconditionally.

2. Variation of slip velocity

To establish the condition under which the vapor-phase velocity might decrease faster than the droplet velocity ($dV_g/dV_l > 1$), we again refer to the expression for dV_g/dV_l as obtained earlier [Eq. (B4)]. Once again, it is stressed that all quantities in Eq. (B4) correspond to those downstream of the frozen shock. If they are expressed in terms of the upstream conditions with the help of standard shock relations, then the condition for $dV_g/dV_l > 1$ becomes

$$\frac{y_1}{1 - y_1} \left(1 - \frac{\gamma - 1}{\gamma} \cdot \frac{(\gamma + 1)M_{f1}^2}{(\gamma - 1)M_{f1}^2 + 2} \right) > \frac{1}{\gamma} \left(\frac{2\gamma M_{f1}^2 / (\gamma - 1) - 1}{M_{f1}^2 + 2 / (\gamma - 1)} - 1 \right), \quad (B6)$$

which, on simplification, reduces to

$$M_{f1}^2 < [\gamma + 1 + y_1(\gamma - 1)] / (\gamma + 1 - 2y_1). \quad (B7)$$

As a typical example, we take $\gamma = 1.32$ and $y_1 = 0.1$, and the above relation then gives $M_{f1} < 1.053$. If interphase heat transfer were taken into account, the limiting Mach number would be slightly higher than that given by Eq. (B7).

3. Variation of wetness fraction

As shown in Sec. V A, $dy > 0$, if $dV_g/V_g > dV_l/V_l$. The condition $dV_g/V_g > dV_l/V_l$ may, again with the help of Eq. (B4), be expressed as

$$[y_1 / (1 - y_1)] (\gamma + 1) M_{f1}^2 [2\gamma - (\gamma - 1) M_{f1}^2] > [(\gamma + 1) M_{f1}^2 - \gamma - 1] [(\gamma - 1) M_{f1}^2 + 2]. \quad (B8)$$

On simplification, it may be shown that the critical Mach number for this condition to hold is given by the root of the equation

$$(\gamma - 1) M_{f1}^4 + [(3 - \gamma)(1 - y_1) - 2y_1\gamma] M_{f1}^2 - 2(1 - y_1) = 0. \quad (B9)$$

For $\gamma = 1.32$ and a typical upstream wetness fraction of 0.1, this critical Mach number is found to be 1.058. That this critical Mach number is not very different from the limit

derived in the previous subsection above is due to V_1 being nearly equal to V_g in this limit.

APPENDIX C: LINEAR THEORY WITH COMBINED VELOCITY AND VAPOR THERMAL RELAXATION

For a linearized analysis, it is possible to obtain an analytical solution for simultaneous velocity and thermal relaxation, even though the relaxation times are of quite different magnitudes. (In fact, the analysis can be extended to include droplet temperature relaxation, but the extra complexity is hardly justified.)

Equilibrating the droplet temperature ($\Delta T/\tau_D \rightarrow V_1 dT_g/dx$) and neglecting second-order terms, the rates of change of ΔT and ΔV in the relaxation zone can be derived from the conservation and the interphase transfer equations [Eqs. (10)–(15)]. The expressions to be solved are

$$(1-M_{e1}^2) \frac{1}{T_g} \frac{d\Delta T}{dx} + (1-M_{e3}^2) \frac{\Delta T}{V_g \tau_T T_g} = \frac{V_g^2}{c_p T_g} \left(1 - \frac{c_p T_g}{h_{fg}}\right) \frac{y}{1-y} \frac{\Delta V}{V_g \tau_I V_g}, \quad (C1)$$

$$(1-M_{e1}^2) \frac{1}{V_g} \frac{d\Delta V}{dx} + (1-M_{e2}^2) \frac{\Delta V}{V_g \tau_I V_g} = \left(1 - \frac{c_p T_g}{h_{fg}}\right) \frac{\Delta T}{V_g \tau_T T_g}, \quad (C2)$$

where M_{e1} , M_{e2} , and M_{e3} are the Mach numbers corresponding to the different equilibrium sound speeds a_{e1} , a_{e2} , and a_{e3} , as defined in Ref. 9 (i.e., $M_{e1} = V_g/a_{e1}$, $M_{e2} = V_g/a_{e2}$, etc.). These equilibrium sound speeds are derived subject to different thermal and mechanical constraints. Here, a_{e1} corresponds to droplet temperature equilibration but frozen momentum and heat transfer, a_{e2} corresponds to equilibrium droplet temperature and velocity slip but frozen heat transfer, and a_{e3} corresponds to the full-equilibrium flow. As a typical example, the ratios of different sound speeds for wet steam at 1 bar and 0.1 wetness fraction are given by

$$a_f : a_{e1} : a_{e2} : a_{e3} \equiv 1 : 0.996 : 0.945 : 0.89.$$

Equations (C1) and (C2) are coupled differential equations for the variables ΔV and ΔT and could easily be solved analytically if we could linearize the equations, or in other words, if we could assume the coefficients are constant. However, after a weak frozen shock wave, the downstream vapor velocity may be such that one or all of the terms like $(1 - M_{e1}^2)$, $(1 - M_{e2}^2)$, and $(1 - M_{e3}^2)$ may undergo a change of sign through the relaxation zone (as they do in a fully dispersed wave). As an example, again consider wet steam at 1 bar and 0.1 wetness fraction. Assuming that an approximate Prandtl's relation is valid across the frozen shock wave, the vapor velocity downstream of the frozen shock would be less than a_{e3} only if the upstream velocity is more than about 1.1 a_f (since $a_{e3} \approx 0.9 a_f$). Hence, if the upstream velocity is less than about 1.1 a_f , at least one of the aforementioned terms

would change sign in the relaxation zone [the velocity at the far downstream end is always less than local a_{e3} (Ref. 10)] and the linear theory would not be valid. On the other hand, if the frozen shock wave is substantial, the values of $\Delta T/T_g$, $\Delta T'/T_g$, and (especially) $\Delta V/V_g$ may not be negligible at the start of the relaxation zone and the second-order effects involving $(\Delta V/V_g)^2$, etc., dominate the initial stage of relaxation. In this case, Eqs. (C1) and (C2) themselves are not valid, since second-order terms were neglected while deriving them. Additionally, there is the problem of substantial variation of τ_T and τ_I in the relaxation zone as discussed in Sec. V. Thus a linearized analysis for the relaxation zone in a partly dispersed wave in vapor-droplet media would be of limited applicability.

¹ W. G. Vincenti and C. H. Kruger, *Introduction to Physical Gas Dynamics* (Wiley, New York, 1965), Chap. 8.

² A. Guha, "The physics of relaxation processes and of stationary and non-stationary shock waves in vapor-droplet flows," *The 4th International Symposium on Transport Phenomena in Heat and Mass Transfer, ISTEP-4*, Sydney, 14–19 July 1991, edited by J. Reizes (Hemisphere, New York, in press).

³ D. Barschdorff, "Droplet formation, influence of shock waves and in-stationary flow patterns by condensation phenomena at supersonic speeds," *Proceedings of the 3rd International Conference on Rain Erosion and Associate Phenomena* (R.A.E., Farnborough, 1970), pp. 691–705.

⁴ A. Guha and J. B. Young, "Time-marching prediction of unsteady condensation phenomena due to supercritical heat addition," *Proceedings of the Conference on Turbomachinery: Latest Developments in a Changing Scene*, London, IMechE Paper No. C423/057, pp. 167–177, 1991.

⁵ F. E. Marble, "Some gas dynamic problems in the flow of condensing vapors," *Astronaut. Acta* **14**, 585 (1969).

⁶ R. Jackson and B. J. Davidson, "An equation set for non-equilibrium two-phase flow, and an analysis of some aspects of choking, acoustic propagation, and losses in low pressure wet steam," *Int. J. Multiphase Flow* **9**, 491 (1983).

⁷ A. Konorski, "Shock waves in wet steam flow," *Pr. Inst. Mech. Precyz.* **57**, 101 (1971) (*Trans. Inst. Fluid Flow Mach., Poland*).

⁸ F. Bakhtar and F. H. Yousif, "Behaviour of wet steam after disruption by a shock wave," *Symposium on Multi-phase Flow Systems*, University of Strathclyde, Institute of Chemical Engineers Paper No. G3, 1974.

⁹ J. B. Young and A. Guha, "Normal shock wave structure in two-phase vapor droplet flows," *J. Fluid Mech.* **228**, 243 (1991).

¹⁰ A. Guha, "Jump conditions across normal shock waves in pure vapor-droplet flows," to appear in *J. Fluid Mech.*

¹¹ E. Becker and G. Böhme, in *Nonequilibrium Flows*, edited by P. P. Wegener (Marel Dekker, New York, 1969), Vol. 1, Chap. 2.

¹² N. H. Johannesen, H. K. Zienkiewicz, P. A. Blythe, and J. H. Gerrard, "Experimental and theoretical analysis of vibrational relaxation regions in carbon dioxide," *J. Fluid Mech.* **13**, 213 (1962).

¹³ A. H. Nayfeh, "Shock-wave structure in a gas containing ablating particles," *Phys. Fluids* **12**, 2351 (1966).

¹⁴ G. Rudinger, "Some properties of shock relaxation in gas flows carrying small particles," *Phys. Fluids* **7**, 658 (1964).

¹⁵ H. W. J. Goossens, J. W. Cleijne, H. J. Smolders, and M. E. H. van Dongen, "Shock wave induced evaporation of water droplets in a gas-droplet mixture," *Exp. Fluids* **6**, 561 (1988).

¹⁶ P. Roth and R. Fischer, "An experimental shock wave study of aerosol droplet evaporation in the transition regime," *Phys. Fluids* **28**, 1665 (1985).

¹⁷ A. Guha, "The fluid mechanics of two-phase vapor-droplet flow with application to steam turbines," Ph.D. thesis, University of Cambridge, 1990.